ESRF	**Experiment title:** x-ray tomography measurements on lymphocytes T using CdSe quantum dotsas contrast reagents	**Experiment number**: **MA-302**
Beamline:	**Date of experiment**: from: 04 July 2007 to: 10 July 2007	**Date of report**: 11/14/2008
Shifts:	**Local contact(s)**: Dr. Peter CLOETENS	*Received at ESRF:*

Names and affiliations of applicants (* indicates experimentalists):

Prof. Daniele FIORETTO, Università di Perugia

Dr. Peter CLOETENS, ESFR

Dr. Silvia COREZZI, Università di Perugia

Prof. Carla EMILIANI, Università di Perugia

Dr. Simona MENCARELLI, Università di Perugia

Report:

We performed intracellular labeling with a mouse primary antiboby specific for β-tubulin, a protein associated with cytoskeleton microtubules, followed by a goat anti-mouse IgG conjugated to Qdot® 605 (CdSe/ZnS core-shell QD). Labeled cells were then included in epoxy resin and resin slices, about 60 nm thick, were attached to Si_3N_4 windows. A single cell was raster scanned with incident X-ray energy of 17.5 keV. Pixel by pixel analysis of the elements present in the core-shell of QDs (S, Zn, Cd, and Se) can be used to retrieve a topographical map of their intracellular distribution (Fig.1). It can be seen that the emission intensity of Zn and S, the elements that also constitute the shell of the QDs, is mainly located in the nuclear region, although a clear signal can be detected also in the cytoplasm. The relatively high concentration of these elements and their presence in both the test and the control sample suggest that the main contribution to the detected signal comes from the elements naturally present into the cell. On the other hand, the Cd signal is almost undetectable, while the Se signal is clearly detected only in the cytoplasm of the labeled sample, while it is not present either in the cytoplasm or in the nucleus of the control sample. Even if the microtubule structure can not be seen since they are 25 nm diameter polymers that course throughout the cytoplasm, this observation is consistent with a higher concentration of Se in the cytoplasm due to the specific binding of the secondary antibody conjugated to QDs to the primary antibody that recognizes the microtubule-associated protein β-tubulin. The cytosolic distribution of the XRF Se map suggests selenium to be a very good marker for the presence of QDs. As a matter of fact, a look at the emission spectra reveals that the Kα line of Se is not in close proximity to other emission bands assigned to biologically relevant elements. This is the ideal condition for obtaining a reliable map of this element. One could object that Se is already present in untreated cells since it is an essential trace element for animals and humans. However, the very low levels of this oligoelement are not sufficient to give a detectable cytoplasmatic signal in the control specimen, confirming that the signal in the test sample comes from QDs. An important proof of this hypothesis comes from the quantitative analysis of the density of Se inside the cell. In fact, the Se map in Fig.1 shows a density of about 0.6-1.3 10^{-4}g/cm^3 in a pixel of 100x100x60 nm^3, corresponding to 4-8 10^{-20} g of Se inside a single pixel. This value can be compared with 1.3 10^{-19} g, the nominal mass of Se in a single QD. Considering that the position of a QD does not necessarily coincide with the center of a pixel, the values are consistent with the idea that single QD's are causing the measured signal per pixel. A second proof should come from the density of Cd which is expected to mirror that of Se. To this respect, Fig.1 shows an unexpected high nominal density of Cd of about 0.01 g/cm^3 in single pixels, completely uncorrelated with the position of the cell. This looks more like noise than a true elemental distribution. A possible reason for this fact can be found in the poor efficiency of the L-lines of Cd (between 2.77 and 3.95 keV), and their coincidence with the K-lines of Ar and Ca, whose strong intensity prevents a reliable detection of the signal from Cd.

To avoid possible problems of elemental redistribution associated with resin inclusion procedure, we explored the suitability to grow cells directly on Si_3N_4 membranes. Viability tests of SKOV3 cells grown on this substrate

showed neither cytotoxic effects nor morphological alterations. In addition, there was no necessity to improve cell adherence. Si_3N_4 membrane windows were sterilized by 30 min UV treatment before the cells were seeded, grown to 60% confluence, and treated according to a standard immunohistochemical protocol as described in Section 2. We thus performed cell surface labeling by incubating sequentially the cells with a mouse anti-HER2 primary antibody and goat anti-mouse IgG conjugated to Qdot® 605. For S-XRF, labeled cells were dehydrated in ethanol and dried at RT just before the measurement. Figure 2 shows the nanoXRF results on surface labeled cells.

Despite a poorly preserved cell morphology due to the prolonged dehydration at RT, the pixel by pixel nanoXRF area density maps of Cd, Se, Zn and S in QD-labeled and control cells, again demonstrate that the Se signal clearly reproduces the QD cell surface distribution that can also be seen by confocal microscopy analysis. The quantitative analysis of Se content on the cell surface allows one to estimate the concentration of QDs. It can be seen that the surface density of Se in a single 100x100 nm^2 pixel inside the perimeter of the cell is about 0.002-0.003 $\mu g/cm^2$, which corresponds to 2-3 10^{-19} g of Se in a single pixel. Similar to the case of intracellular labeling, this value is very close to the mass of a single QD. Also in this case, the signal from Cd is not reliable and Se stands out as the key element for mapping the position of QDs. This result clearly demonstrates the suitability of S-XRF with QDs labeling for surface mapping of target proteins.

Along with elements included in the QD core-shell, a wide range of biologically relevant elements can be quantitatively imaged with X-ray excitation at 17.5 keV. Figs. 1 and 2 display a selection of two-dimensional quantitative elemental maps that were obtained simultaneously from the hyperspectral XRF imaging of specimens either included in epoxy resin or dehydrated in graded ethanols and dried at RT.

The region of the nucleus is clearly distinguished from that of cytoplasm in Fig.1. Nucleoli are nicely evidenced as bright round structures inside the nucleus in the maps of Ca and Zn and are also visible in the maps of other elements. This result suggests that S-XRF can be used to study the nuclear structure in different conditions of cellular growth and differentiation, both in physiologic and pathologic conditions.

When studying the subcellular distribution of diffusible anions or metal cations, it is important to consider how the specimen preparation might affect the intracellular concentration of these elements. For example, while some elements are presumably tightly bound to endogenous ligands, either proteins or small molecules, the concentration of other elements is expected to change significantly upon cell membrane permeabilization and extensive washing as required in standard immunohistochemical protocols. We observed that the Cl signal is higher in the samples included in the epoxy resin (Fig.1) than in samples dried at RT (Fig.2). It has to be considered that the protocol for epoxy resin inclusion requires additional passages and chemicals and that the resin itself contains a small percentage of Cl. On the other hand, samples dehydrated with ethanol dried at RT under ambient atmosphere are not able to preserve the cell morphology, like samples included in resin are able to do. These latter are not subject to degradation, can be stored for months at RT and re-examined after a long period.

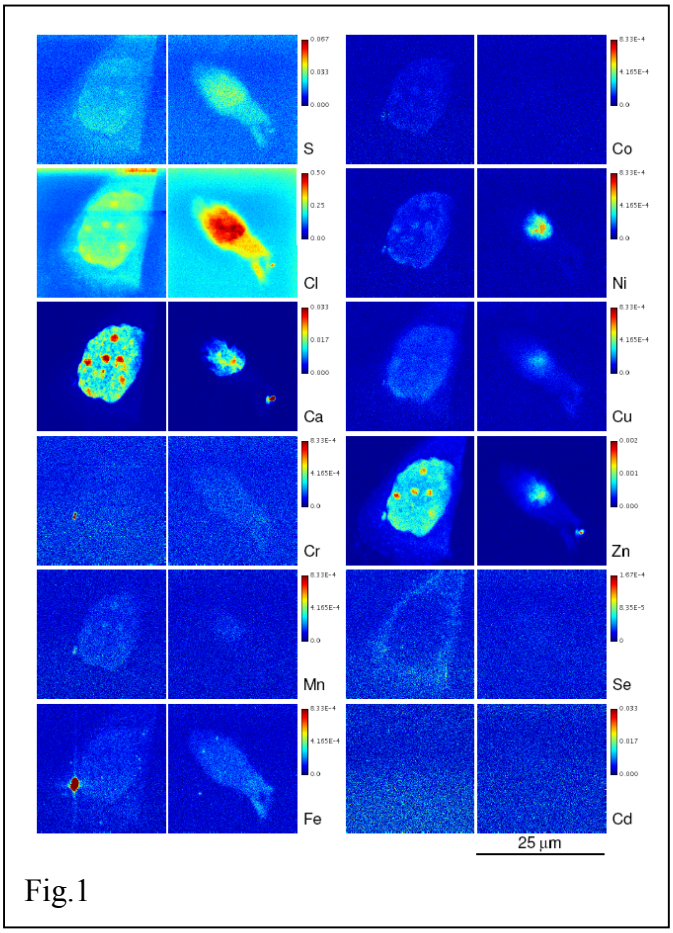

Fig.1

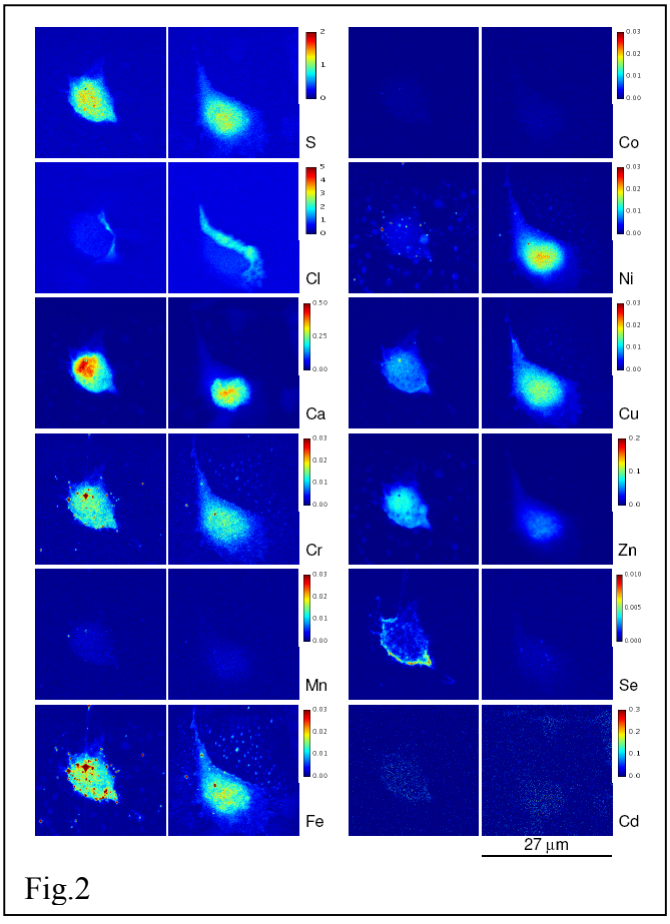

Fig.2